Available online at www.sciencedirect.com
ScienceDirect
Biosensors and Bioelectronics xxx (2008) xxx–xxx
BIOSENSORS & BIOELECTRONICS
www.elsevier.com/locate/bios

# Percutaneous fiber-optic sensor for chronic glucose monitoring *in vivo*

Kuo-Chih Liao [1], Thieo Hogen-Esch [2], Frances J. Richmond [3], Laura Marcu [4], William Clifton [5], Gerald E. Loeb *

*Alfred E. Mann Institute for Biomedical Engineering, University of Southern California, Los Angeles, CA 90089, USA*

Received 7 August 2007; received in revised form 19 December 2007; accepted 3 January 2008

**Abstract**

We are developing a family of fiber-optic sensors called Sencils™ (*sen*sory *cil*ia), which are disposable, minimally invasive, and can provide *in vivo* monitoring of various analytes for several weeks. The key element is a percutaneous optical fiber that permits reliable spectroscopic measurement of chemical reactions in a nano-engineered polymeric matrix attached to the implanted end of the fiber. This paper describes its first application to measure interstitial glucose based on changes in fluorescence resonance energy transfer (FRET) between fluorophores bound to betacyclodextrin and Concanavalin A (Con A) in a polyethylene glycol (PEG) matrix. *In vitro* experiments demonstrate a rapid and precise relationship between the ratio of the two fluorescent emissions and concentration of glucose in saline for the physiological range of concentrations (0–500 mg/dl) over seven weeks. Chronic animal implantation studies have demonstrated good biocompatibility and durability for clinical applications.


*Keywords:* Optical fiber; Chemical sensor; Fluorescence resonance energy transfer; Affinity-binding assay; Glucose; Quantum dots

## 1. Introduction

Clinical studies have concluded that fine-tuning of insulin administration on the basis of frequent glucose measurements provides substantial advantages in the management of diabetes (Diabetes Control and Complication Trials Research Group, 1993; UK Prospective Diabetes Study Group, 1998). Such treatment can dramatically reduce mortality and complications from the chronic metabolic fluctuation in either hyperglycemia or hypoglycemia. Ideally, insulin could be administered by "artificial pancreas" consisting of a chronically implantable sensor, a pump and an algorithm to adjust dosage continuously.

Presently, insulin delivery technology (insulin formulation and pump designs) is well developed but glucose sensors remain problematic (Steil et al., 2004). A suitable sensor should have a low cost to operate, which is related to the cost of the sensor itself, the cost to install it and the frequency at which it must be changed. It should be ergonomically unobstructive and easy to use to facilitate frequent measurements. It must have sufficient accuracy (as defined clinically by error grid analysis; Clarke, 2005), ideally without requiring intrusive calibration.

In the current clinical environment, choices for glucose monitoring are limited. Intermittent self-monitoring of blood glucose (SMBG) is the clinical method of choice. Typically, glucose measurements are done by pricking a finger (or other more insensitive region such as upper arm) and extracting a drop of blood, which is then applied to a test strip composed of chemicals sensitive to the glucose in the blood sample. An optical meter is used to analyze the blood sample and gives a numerical glucose reading. Most conventional SMBG devices have 95–99% accuracy in Clarke error grid analysis (Clarke, 2005). Because of the associated pain and inconvenience, however, few patients take more than a couple of readings per day, and so are at risk from unexpected and undetected peaks and valleys of glucose

* Corresponding author at: AMI-USC, DRB-B11, 1042 Downey Way, Los Angeles, CA 90089-1112, United States. Tel.: +1 213 821 1112; fax: +1 213 821 1120.
*E-mail address:* gloeb@usc.edu (G.E. Loeb).
[1] Present address: 12F-1, No. 86, Sec. 1, Huamei W. Street, West District, Taichung City, Taiwan.
[2] Present address: Department of Chemistry, University of Southern California, CA, USA.
[3] Present address: School of Pharmacy, University of Southern California, CA, USA.
[4] Present address: Department of Biomedical Engineering, University of California at Davis, CA, USA.
[5] Present address: Baylor College of Medicine, Houston, TX, USA.

0956-5663/$ – see front matter © 2008 Elsevier B.V. All rights reserved.
doi:10.1016/j.bios.2008.01.012

concentrations. The FDA has conditionally approved 4 short-term (<72 h) continuous monitoring sensors. All measure interstitial fluid glucose concentrations using the long-established enzymatic method involving glucose oxidase. This assay method consumes glucose enzymatically, creating a concentration gradient that may become steeper as the sensor is walled-off by the foreign body reaction. The glucose oxidase deteriorates over time and is sensitive to pH and temperature (Usmani and Akmal, 1994; Tamada et al., 2002; Wentholt et al., 2006). Limited or uncertain stability and accuracy (<80% in Clarke error grid analysis) prevent them from being used exclusively, so patients must still calibrate and cross-check using SMBG methods. The percutaneous probes are inherently complex and expensive to manufacture and include a multipin electrical connector that must be fixed mechanically to the skin surface near the point of entry. This fixation interferes with physical activity and hygiene and itself limits the long-term use of such percutaneous sensors.

We are developing a family of disposable, minimally invasive, *in vivo* sensors that can measure various analytes in a patient over a period of several weeks. The key element is a chronically implanted optical fiber (Fig. 1) with size and flexibility similar to a human hair, which would enable it to be both mechanically stable and unobtrusive when implanted in any convenient patch of hairy skin. Optical fibers are thin, lightweight, chemically stable, and generally biocompatible, all desirable properties for medical devices. Fiber communication technology is well established and has the advantages of high capacity, low attenuation, immunity to electromagnetic interference, and inherent electrical isolation that are attractive for this application.

The glucose sensor measures glucose concentration by the much-studied fluorescence resonance energy transfer (FRET) assay based on the selective binding of saccharides by the

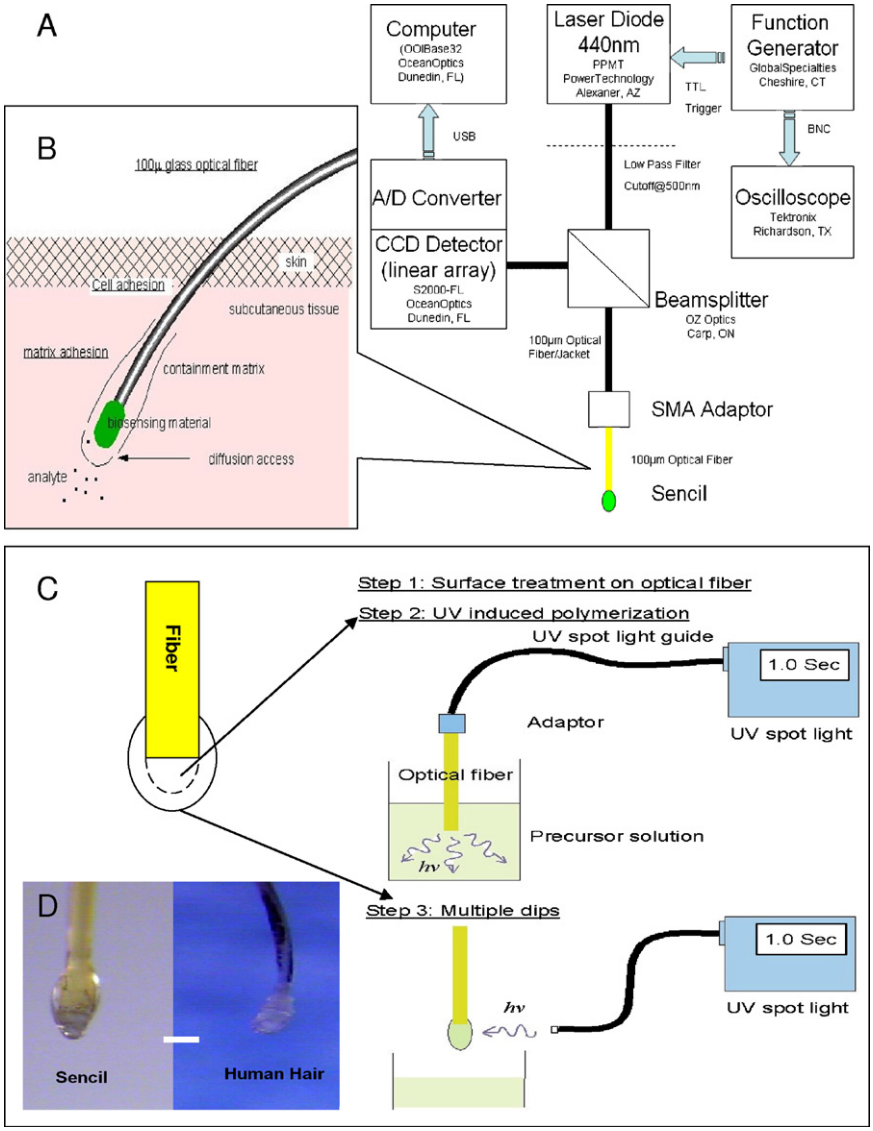


Fig. 1. Basic components and fabrication of Sencil prototype. (A) Laboratory spectroscopic instrumentation used to test prototypes; similar functionality must be miniaturized for portable clinical reader. (B) Sensor components and relationships to tissue *in vivo*. (C) Scheme of manufacture method with adhesion enhancement. (D) Similarity of shape and size between Sencil and human hair with attached follicle (white bar = 100 μm).

Please cite this article in press as: Liao, K.-C., et al., Biosens. Bioelectron. (2008), doi:10.1016/j.bios.2008.01.012

jack bean lectin Concanavalin A (Con A)(Meadows and Shultz, 1993). We have reengineered the chemistry, however, to overcome the challenges of chemical sensing *in vivo*:

In order to obtain sufficiently strong fluorescence from a very small sensor volume, it is necessary to incorporate fluorophores at high concentration, but that tends to increase the concentration of glucose required for competitive binding to affect FRET. Replacing linear dextran with betacyclodextrin (which has lower affinity for Con A) allowed us to improve the signal-detection sensitivity 60-fold, while preserving glucose-concentration sensitivity in the physiological range of 0–500 mg/dl (Liao et al., 2005).

In order to take full advantage of the simplicity of a single, percutaneous optical fiber, the fluorescence signals must be split and filtered from the much brighter excitation light. Quantum Dots (Qdot) can be excited at any wavelength shorter than their emissions, whereas organofluorophores such as fluorescein isothiocyanate (FITC) must be excited at a specific wavelength fairly close to their emission. Qdots also have a higher quantum yield, making them suitable for the FRET donor (but not the FRET acceptor). Preliminary results were presented by Liao et al. (2006).

Concentration of glucose is inferred from the ratio of the two fluorescent emissions at 525 nm and 570 nm rather than the absolute intensity of either. The preliminary results confirmed that it makes the assay relatively insensitive to variability of the photonic coupling or deterioration of the sensing materials over time. Because the assay is a reversible binding reaction, it does not consume glucose as does glucose oxidase. Encapsulation by a diffusion barrier of connective tissue might slow the dynamic

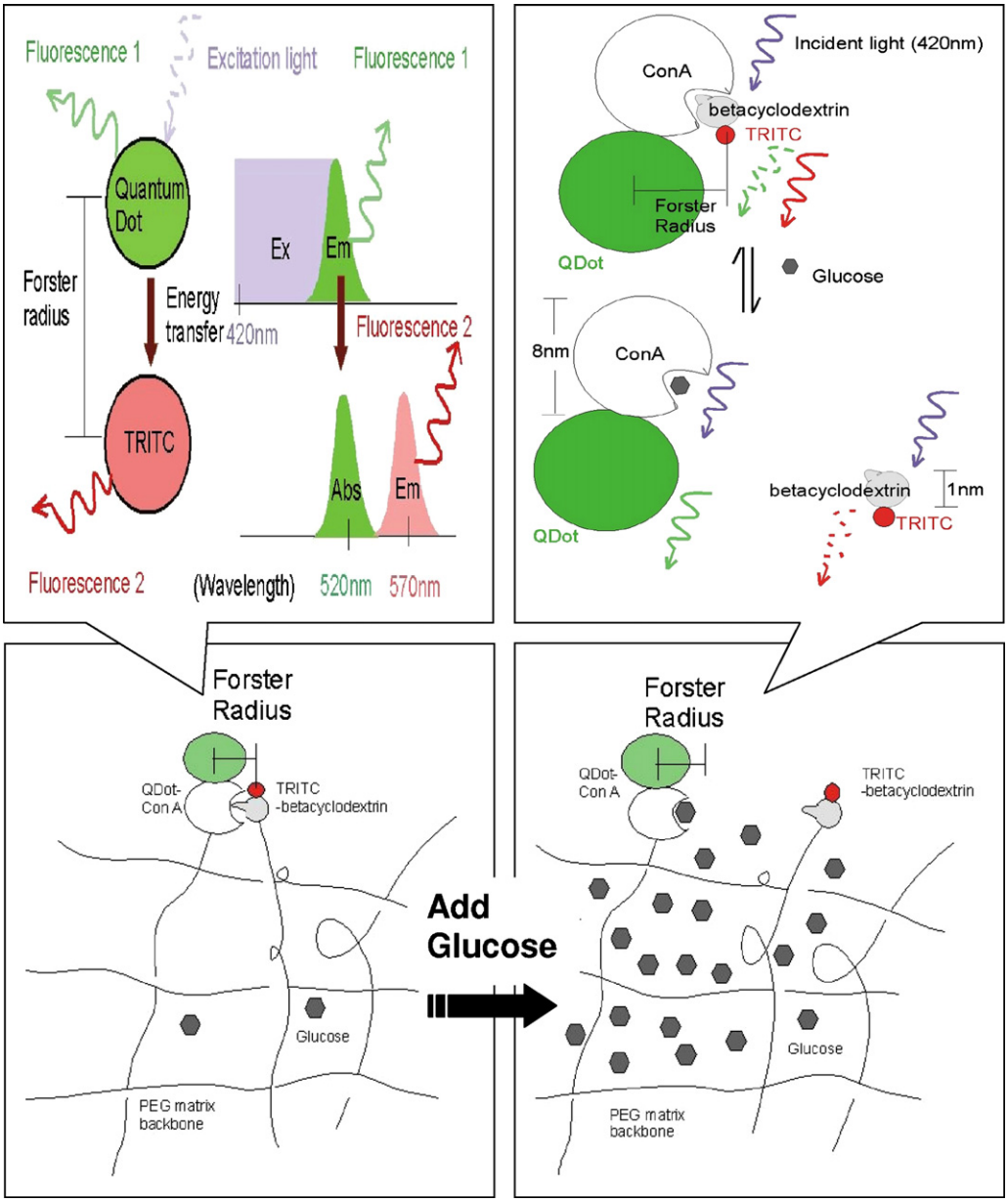


Fig. 2. Illustration of glucose assay system. Changes in FRET between fluorophores covalently immobilized on the flexible PEG matrix depend on changes in the distance between them, which in turn depends on the competitive natural affinity between Con A and various saccharides such as betacyclodextrin and glucose.

Please cite this article in press as: Liao, K.-C., et al., Biosens. Bioelectron. (2008), doi:10.1016/j.bios.2008.01.012

responses of the sensor but would not be expected to produce a false concentration gradient around the detection site. The principles of the assay are illustrated in Fig. 2 and described in the "Supplementary Material" section.

The chronic biocompatibility and mechanical integrity of Sencil for in vivo application have been evaluated by animal studies. Histology of chronically implanted sites has verified the biocompatibility of the Sencil. Very small quantities of PEG (approximately 10 μg) and Con A ($<10^{-12}$ g/Sencil) may be left behind if the matrix detaches when the spent Sencil is plucked out (Liao et al., 2005), but this should have negligible effects even cumulatively (the lethal dose of Con A in mice is 50 mg/kg by intravenous injection).

The polyimide coat of the optical fiber improves its mechanical toughness greatly, but it discourages cell and protein adhesion (Tan et al., 2001; Drumheller and Hubbell, 1994), which are needed for percutaneous fixation. The optical fibers separated easily from the PEG matrix and tended to slip out of the skin. To address both problems, we decided to bind a layer of collagen covalently to the polyimide coating because collagen is a well-known cell adhesion promoter (Darwin and Kivirikko, 1995; Jokinen et al., 2004) and it can be cross-linked to the PEG matrix (Liao et al., 2006).

In this study we demonstrate the *in vitro* performance of the prototype sensor, and summarize the improvement of chronic stability with collagen coated adhesion enhancement *in vivo*.

## 2. Experimental

### 2.1. Reagents and materials

All chemicals involved were purchased from Sigma (St. Louis, MO). Tetramethylrhodamine isothiocyanate (TRITC) and 1-ethyl-3-(3-dimethylaminopropyl)carbodiimide, hydrochloride (EDAC) was purchased from Invitrogen (Carlsbad, CA). α-acryloyl, ω-*N*-hydroxysuccinimidyl ester of poly (ethylene glycol)-propionic acid, MW 3400 (PEG-NHS 3400) was purchased from Shearwater Inc. (Huntsville, AL). The silica optical fiber was purchased from OceanOptics with 100 μm core, 110 μm cladding and 10–25 μm thick polyimide coat. All other reagents were analytical grade and used without further purification. All aqueous solutions were prepared with doubly distillated water.

### 2.2. Fabrication of Sencil probe

#### 2.2.1. TRITC-betacyclodextrin conjugation and modification

We used the isothiocyanate reaction to conjugate TRITC to betacyclodextrin. Betacyclodextrin was dissolved in dimethylsulphoxide containing a few drops of pyridine. TRITC was added, followed by dibutyl tin dilaurate, and the mixture was heated for 2 h at 95 °C. The TRITC-betacyclodextrin was dried by reduced pressure evaporation to remove solvent (De Belder, 1973). The residue was dissolved in phosphate buffered saline (PBS). Dialysis and fluorescence measurements on the dialysate were used to separate unbound fluorophore and quantify the stoichiometry of the bound fluorophore.

The TRITC-labeled betacyclodextrin had a molecular weight of 1 kDa, which is 1800 times reduced in size compared to the molecule that Meadows and Schultz immobilized by trapping in PEG. This small dextran is unlikely to be trapped effectively in the PEG matrix. Therefore, we modified the labeled betacyclodextrin with an acryloyl group, which provides a covalent binding site to attach the molecule to the PEG matrix. A solution of acryloyl chloride (0.54 g, 6 mmol) in 10 ml $CH_2Cl_2$ was added dropwise to a solution of TRITC-betacyclodextrin (3 mmol) and triethylamine (3.2 g, 31.7 mmol) in 60 ml $CH_2Cl_2$ at −5 °C over 1 h. The reaction mixture was stirred over night at room temperature, and then triethylamine hydrochloride was filtered off. The filtrate was diluted with 100 ml $CH_2Cl_2$ and extracted with 2 × 50 ml $NaHCO_3$ (10%) and 1 × 50 ml brine. The organic phase was dried over $MgSO_4$, filtered and distilled to give crude product (Sha et al., 2003). The effectiveness of the binding was assayed by measuring the fluorescence of the supernatant after prolonged soaking in PBS.

#### 2.2.2. Qdot–Con A conjugation

Five milligrams Con A was dissolved in 10 ml borate buffer with 20 mg succinic anhydride for 2 h (Gunther et al., 1973). Dithiopthrethiol (DTT) was added to reduce the thiol group of Con A with the final concentration at 20 mM, and kept in room temperature for 30 min. 4-(Maleimidomethyl) cyclohexanecarboxylic acid *N*-succinimidyl ester (SMCC) was used to activate Quantum Dot in DMSO with the final concentration at 1 mM, and reacted in room temperature for 1 h. Size exclusive columns packed with Sephadex$^{TM}$ G-25 medium were used to remove excess DTT and SMCC. The activated Qdot was treated with caprylic acid N-succinimidyl ester. Both activated materials reacted for 1 h in room temperature. The reaction was quenched by betamercaptoethanol. The Qdot-Con A was separated by size-exclusive columns packed with Superdex 200 gel.

#### 2.2.3. Collagen coating treatment for adhesion enhancement

The optical fiber was treated in 4 M potassium hydroxide for 3 h and washed by pH 5 phosphate buffer. The etched fiber was activated for 15 min in a solution with both 50 mg/ml EDAC and 50 mg/ml *N*-hydroxysuccimide dissolved in pH 5 buffer. The activated fiber was washed with pH 5 buffer and reacted with 1 mg/ml collagen for 2 h. Then the collagen coated fiber was washed with pH 7.4 PBS and activated with 10 mg/ml NHS-PEG-acrylate dissolved in pH 7.4 PBS.

#### 2.2.4. Hydrogel precursor solution preparation

UV induced polymerization is used to attach the biosensing matrix to the internal end of the fiber. In order to immobilize Con A, a trace amount of PEG-NHS 3400 was added into the precursor solution (1/200 mass ratio to PEG-DA) and incubated with Con A for 30 min. The NHS ester of NHS-PEG-diacrylate reacted with lysine residue on the surface of Con A to form

Please cite this article in press as: Liao, K.-C., et al., Biosens. Bioelectron. (2008), doi:10.1016/j.bios.2008.01.012

a covalent bond. Another acrylate end-group of NHS-PEG-acrylate was crosslinked with PEG-DA to form the hydrogel matrix during UV-induced polymerization (Russel et al., 1999).

The precursor solution of the polymer matrix was prepared with 1 ml PEG-DA, 5 mg NHS-PEG-acrylate, and 0.5 ml of 10 nM Qdot-Con A (Conjugation method is described in Section 2.2.1) and 30 nM TRITC-betacyclodextrin (Conjugation method is described in Section 2.2.2) in PBS. After vortexing for 30 min, 100 μl of trimethylolpropane triacrylate (TPT) and 10 mg of 2,2-dimethoxy-2-phenylacetophenone (DMPA) were added to the solution, and vortexed for another 30 min.

### 2.2.5. Sensor probe assembly

The hydrogel is polymerized and attached onto the end of an optical fiber using the novel process illustrated in Fig. 1C. The polyimide jacket of the optical fiber is etched with potassium hydroxide and covalently coated with collagen as described in Section 2.2.3. The coated fiber is then dipped into precursor solution (Section 2.2.4) and UV light is applied through the fiber to polymerize the hydrogel on the end. The dimension of the hydrogel can be adjusted precisely by setting the duration and intensity of UV light exposure. Multiple dip-coats are used to build up the desired size and shape, and increase the interface area for adhesion of the matrix along the shank of the fiber. Each successive layer is polymerized by UV light directed onto the outside of the fiber. These processes can be readily scaled and automated for industrial manufacture at low cost.

### 2.2.6. Sterilization

The Sencils were immersed in 70% ethanol overnight. The devices were removed from the ethanol solution and allowed to dry in a sterile pouch for another 24 h before implantation. Industrial fabrication under sterile conditions is feasible; other methods of sterilization are under investigation.

## 2.3. Configuration of Sencil prototype

Bench instrumentation using off-the-shelf components is illustrated schematically in Fig. 1A. A 45 mW laser diode (Power Technology, Alexander, AZ) produced the excitation at 440 nm. The excitation light was conveyed through the 10% arm of a custom 90/10 beamsplitter (OZ Optics, Carp, ON) to reach the Sencil through a 120 μm SMA (industry standard Sub Miniature version A) adapter (OceanOptics, Dunedun, FL). The returning fluorescence signal went through the beamsplitter and was directed to the detector S-2000FL (OceanOptics, Dunedun, FL) via the 90% arm of the beamsplitter. This detector has a grating to spread the light at different angles onto a 2048-element CCD linear array according to its wavelengths. Each CCD element records the photon count at a corresponding wavelength as an analog signal. The analog signal is digitized and processed on a desktop computer installed with OOIBase32 software through a USB connection.

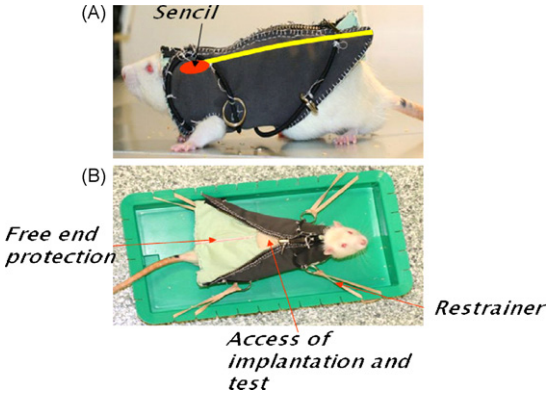


Fig. 3. Jacket designed to protect implanted Sencils during chronic experiments in rats. (A) Jacket in place on freely moving rat; red oval shows approximate site of injection and yellow line shows approximate course of guide tube in which the free end of the Sencils was free to slide (both inside jacket). (B) Jacket used as a restraint during measurement of retention force, unzipped to reveal the implantation site and guide tube (For interpretation of the references to color in this figure legend, the reader is referred to the web version of the article).

## 2.4. Sensor prototype test methods

### 2.4.1. Verification of adhesion enhancement and chronic integrity with surface treatment

Six Sprague Dawley rats (350–550 g) were implanted with control Sencils (two each) and collagen-coated Sencils (four each). Those rats were adapted to and wore a jacket at all times to protect the Sencil from damage from their aggressive grooming and daily activity (Fig. 3A). The jacket also served as a restrainer when tied on a surgery board with rubber bands (Fig. 3B) so that the animal itself was not traumatized by the restraint. We implanted the Sencil near the back of the neck and shoulder blade through an opening in the jacket. The jacket included foam spacers to keep the fabric from abrading the Sencils at their entry into the skin and a sheath (soda straw) in which the external ends were free to slide. The force required to pull a sensor probe from the skin was determined by clamping the external end of the fiber in the padded jaws of the peak-force meter and slowly pulling until it was removed completely (*in vivo* pull test). The extracted sensor probes were also examined under a light microscope to determine whether the matrix was still attached to the intenal end of the optical fiber.

### 2.4.2. Study of chronic sensor performance in vitro

Sencils were immersed in 100 mg/dl glucose concentration in pH 7.4 PBS. The containers were stored in a 37 °C oven to simulate physiological conditions. The sensors were removed from the oven and placed in glucose-free saline (pH 7.4 phosphate buffer) over night before test.

# 3. Results and discussion

## 3.1. Chronic biointerface integrity with adhesion enhancement

Before we conducted *in vivo* studies in rats, we measured the adhesion enhancement between the sensing matrix and the

Table 1
Summary of chronic stability with adhesion enhancement

| | Sencil with collagen-coated fiber | Sencil with bare fiber |
|---|---|---|
| *In vitro* pull test | 39.0 ± 5.62 ($n$ = 5) | 0.8 ± 0.75 ($n$ = 5) |
| *In vivo* pull test | 22.0 ± 13.02 ($n$ = 7) | 1.3 ± 1.75 ($n$ = 3) |
| Post-implant anchorage rate | 83.3% (20/24) | 25% (3/12) |
| Sencil with intact matrix after plucking from implantation site | 100% (9/9) | 0% (0/3) |

The detected values of pull tests are shown as mean ± S.D. (g); the subject number of each pull test is listed beneath it. The post-implant anchorage rate after 1st week is shown in percentage.

optical fiber *in vitro*. A peak-force meter was clamped to the free end of the Sencil. The sensing matrix bulb was pulled until it separated from the fiber (*in vitro* pull test). We measured a peak tension force of only 0–2 g for untreated 100 μm fibers. Separation force increased to 40 g after collagen treatment. For comparison, 70 g is the mean peak force for removing hair from the human scalp.

Because the surface area of the matrix is small and fibroblasts tend not to adhere well to the hydrogel matrix, we assumed that most of the retention forces of the Sencil to skin would come from interactions along the shank of the optical fiber. In the *in vivo* study, the first pull test was conducted at day 8–9 after implantation. At that time, any acute inflammation from insertion trauma should have subsided and a fibrous capsule should have started to form (Labow et al., 1995). We found that more than 80% (20/24) of the adhesion enhanced devices stayed in place, while less than 30% of (3/12) of the uncoated controls were still present. Subsequent pull tests on samples of the remaining Sencils were conducted at 15th day and 30th day. The extraction force required for collagen-coated Sencils was scattered from 10 to 50 g with a mean of 22 g. The large range appears to be related to heterogeneity in the thickness of the skin and the orientation and depth of the Sencil insertion, which was difficult to control in the thin and flexible skin of the rat. There was no detectable trend over time, suggesting that the implant sites were stable. The extraction force for the uncoated Sencils was generally 0–2 g (one reading exceeded 5 g). The extraction force for nearby hairs was 10.4 g (S.D. 4.1). When we inspected all the collected samples (adhesion enhanced and control Sencils) under the light microscope, the biosensing matrix was still attached to all of the collagen-coated devices but was missing from all of the control devices. The improvement of post-implant anchorage and chronic integrity is summarized in Table 1.

The mechanical stability of the collagen-coated Sencils in rats is encouraging. In contrast to the uncoated Sencils, the PEG matrix appeared to be tightly bound and the force required to extract the Sencil was similar to the force required to extract a normal hair in the rat. It seems likely that the retention forces will be higher for Sencils in the thicker, tougher skin of larger animals such as humans, as they are for normal hairs (70 g in humans vs. 10.4 g in rats). It remains to be demonstrated whether the retention force is actually sufficient to allow Sencils to be placed in exposed skin without requiring bandages or other forms of protection that would reduce their simplicity of use.

### 3.2. Temporal response in vitro

The *in vitro* performance of the prototype sensor was evaluated by spectroscopic measurements while the sensing matrix was placed in glucose solutions with different concentrations at room temperature. Fig. 4B presents the spectral shifts produced as a function of time following exposure to step changes in ambient glucose concentration at room temperature *in vitro*.

The response times of the Sencils to step changes in glucose (Fig. 4B) was only modestly faster than the 10–12 min response times reported for a similar assay performed in 2 mm diameter PEG beads with trapped Con A and saccharide (Russel et al., 1999). Our sensing matrix is about 8 times smaller in diameter

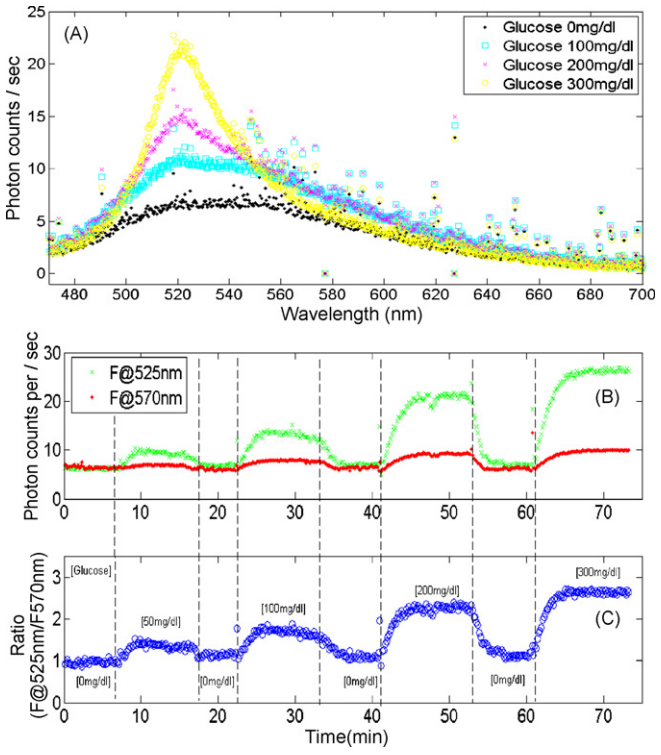


Fig. 4. Dynamic responses of Sencil in different glucose concentrations. (A) Spectra with different glucose concentrations. (B) The green curve indicates the corresponding intensity at 525 nm (theoretical maximal emission wavelength of Qdot-Con A); the red curve indicates the corresponding intensity at 570 nm (theoretical maximal emission wavelength of TRITC-betacyclodextrin. (C) The curve indicates the concentration change of glucose by ratio, which is the emission at 525 nm divided by the emission at 570 nm at each point in time (For interpretation of the references to color in this figure legend, the reader is referred to the web version of the article).

Please cite this article in press as: Liao, K.-C., et al., Biosens. Bioelectron. (2008), doi:10.1016/j.bios.2008.01.012

(250 μm) and should respond more rapidly based on its greater surface area-to-volume ratio. We suspect that binding the Con A and saccharide to the PEG restricts their mobility, so the response time is longer than expected. Also, mobility and diffusion would be higher at body temperature, reducing response time. Fluorescence response time to a decrease in glucose was about 3–8 min. Changing the pore size of the PEG had little effect, suggesting that the limiting factor may be the mobility of the Con A with respect to the betacyclodextrin rather than diffusion of glucose in and out of the matrix. The time-course of fluorescence change at both emission wavelengths (and the ratio between them) was similar in response to step changes in glucose concentration.

### 3.3. Reproducibility and stability over time in vitro

The intensity of fluorescent emissions was stable for the first 6 weeks of incubation in saline at 37 °C but showed a significant decrease starting in week 7 (Fig. 5A). Importantly, the intensity ratio between the two emissions that is used to quantify glucose concentration was preserved even when the absolute intensities were declining (Fig. 5B).

The relationship between glucose concentration and fluorescence ratio (Fig. 5B) was unexpectedly nonlinear even over ranges where saturation was not expected or apparent. This appears to be related to overlap of the two emissions spectra (Fig. 4A), such that the peak amplitudes of each are influenced by the skirts of the other. The problem is exacerbated for high glucose concentrations (>300 mg/dl) in which Qdot fluorescence is less quenched by FRET and the emission peak of TRITC is completely obscured by the Qdot emission. More accurate measurement can be achieved by estimating the area-under-the-curve attributable to each fluorophore and filtered by numerical signal processing tools, such as independent component analysis (ICA). ICA maximizes the degree of statistical independence among outputs using contrast functions. It imposes the criterion that the multivariate probability density function (p.d.f.) of output variables factorizes. Finding such a factorization requires that the mutual information between all variable pairs go to zero (Kenji et al., 2005; Maeda et al., 2001). ICA combined with enhanced signal strength should provide the accuracy and precision required for a clinical glucose sensor.

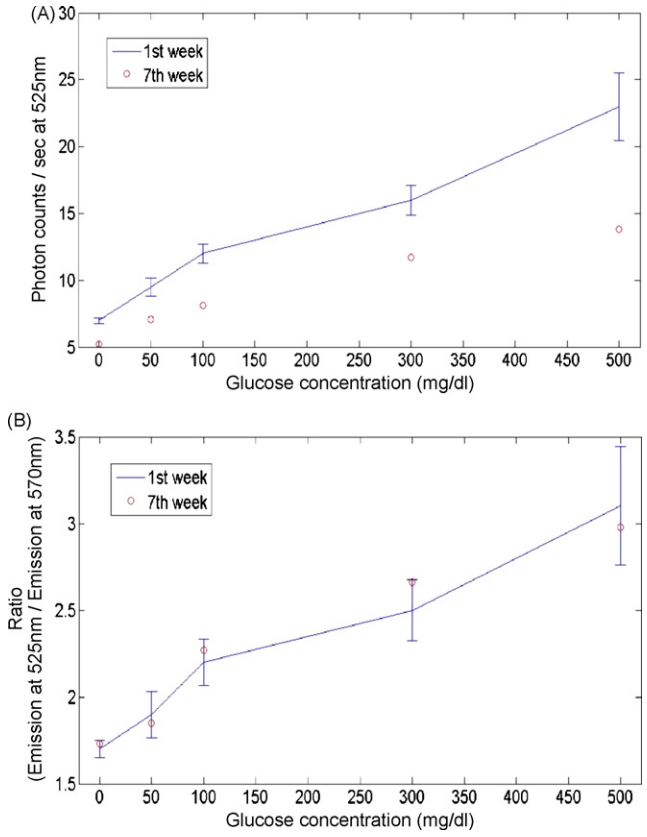


Fig. 5. Effect of PEG matrix degradation over time. (A) The fluorescence intensity of Qdot-Con A at emission maximal wavelength. (B) The ratio of the two fluorescence intensities at emission maximal wavelengths. Error bars indicate standard deviations for measurements in weeks 1–6.

The changes in performance over time were consistent with generalized degradation of the PEG matrix rather than selective changes in the assay itself. If the PEG matrix degrades gradually from the outer surface inward, the intensity of fluorescence would be expected to decline only late in the process because most of the fluorescence arises from the innermost portions of the matrix close to the aperture of the optical fiber. Even then, the ratio of the fluorescence signals (from which the glucose concentration must be estimated) remains stable. Declining intensity of fluorescence would be associated with increased noise (loss of precision) rather than systematic error (loss of accuracy) in glucose estimation and could be used as an indicator that the Sencil is due for replacement.

## 4. Conclusions

The prototype glucose Sencil described here constitutes the first step in the development of a novel class of low-cost chemical sensors suitable for long-term management of ambulatory patients. Key elements of feasibility for glucose sensing can be considered in the context of underlying mechanisms and prior assay development.

The next step toward clinical implementation will be validation of the measurements in chronically implanted animals by comparison with a "gold standard" such as intravenous blood glucose. Key questions *in vivo* include the speed and accuracy over time, the degradation rate of the PEG matrix, and the possible effects of relative motion between the matrix and the surrounding tissues. Before that, however, there are opportunities to enhance the performance of the technology that need to be explored:

- The physical and chemical properties of the polymer matrix can be nano-engineered to alter its hydrophilicity, crosslinking density, pore size, etc. Such changes could improve the ratio of the fluorescent signal to the back-scattered excitation signal and reduce the equilibration time for responses to glucose, which may be important for closed-loop control of insulin administration. These properties may also be important for reengineering the Sencils to be sensitive to other

analytes of interest, many of which have a physiological range of concentrations much lower than glucose.
- The measurement of the fluorescence spectral components would be more accurate if it were based on curve-fitting of the actual spectra of the fluorophores rather than measurements of the photon counts at a single peak wavelength. The spectra in Fig. 4A indicate that the emissions are non-gaussian and overlapped and that noise in the detector is not negligible, suggesting that precision of the measurements could be improved substantially by considering the entire spectral pattern.

Eventually the spectroscopic instrumentation used to couple to the Sencils, excite the fluorophores and separate and measure the fluorescence must be adapted to the limited size and power budget of a portable reader that is simple enough to be used by patients. Recent progress in the integration of photonic, electronic and microelectromechanical (MEMS) systems suggests that this is now feasible.

## Acknowledgements

This research was funded by the Alfred E. Mann Institute for Biomedical Engineering at the University of Southern California. We thank Zhen Wang for assistance with the rat experiments.

## Appendix A. Supplementary data

Supplementary data associated with this article can be found, in the online version, at doi:10.1016/j.bios.2008.01.012.

## References

Clarke, W.L., 2005. Diabetes Technol. Ther. 7, 776–779.
Darwin, J.P., Kivirikko, K.I., 1995. Annu. Rev. Biochem. 64, 403–434.
De Belder, N.A., 1973. Carbohydr. Res. 30, 375–378.
Diabetes Control and Complication Trials Research Group, 1993. N. Engl. J. Med. 329, 977–986.
Drumheller, P.D., Hubbell, J.A., 1994. Anal. Biochem. 222, 380–388.
Gunther, G.R., Wang, J.L., Yahara, I., Cunnungham, B.A., Edelman, G.M., 1973. Proc. Nat. Acad. Sci. 70, 1012–1016.
Jokinen, J., Dadu, E., Nykvist, P., Kapyla, J., White, D.J., Ivaska, J., Vehvilainen, P., Reunanen, H., Larjava, H., Hakkinen, L., Heino, J., 2004. J. Biol. Chem. 279, 31956–31963.
Kenji, K., Shigeru, M., Shinji, U., Yasunori, N., Takanori, K., Shigeru, Y., Shigeru, K., 2005. NeuroImage 28, 669–681.
Labow, R.S., Erfle, D.J., Santerre, J.P., 1995. Biomaterials 16, 51–59.
Liao, K.-C., Hogen-Esch, T., Richmond, F.J., Marcu, L., Loeb, G.E., 2005. Optical Fiber and Sensors for Medical Application V. Proceeding of SPIE 5691, 129–145.
Liao, K.-C., Hogen-Esch, T., Richmond, F.J., Marcu, L., Clifton, W., Loeb, G.E., 2006. Optical Fiber and Sensors for Medical Diagnostic and Treatment VI. Proceeding of SPIE 6083, 60830V.
Maeda, S., Inagaki, S., Kawaguchi, H., Song, W.-J., 2001. Neurosci. Lett. 302, 137–140.
Meadows, D., Shultz, J., 1993. Anal. Chim. Acta 280, 21–30.
Russel, R.J., Pishko, M.V., Gefeides, C.C., Cote, G.L., 1999. Anal. Chem. 71, 3126–3132.
Sha, Y., Shen, L., Hong, X., 2003. Tetrahedron Lett. 43, 9417–9419.
Steil, G.M., Panteleon, A.E., Rebrin, K., 2004. Adv. Drug Deliv. Rev. 56, 125–144.
Tamada, J., Lesho, M., Tierney, M., 2002 April. IEEE Spectrum, 52–57.
Tan, J., Shen, H., Saltzman, W.M., 2001. Biophys. J. 81, 2569–2579.
UK Prospective Diabetes Study Group, 1998. UKPDS 33. Lancet 352, 837–853.
Usmani, A., Akmal, N., 1994. Diagnostic Biosensor Polymers. American Chemical Society, Washington.
Wentholt, I., Hoekstra, J., DeVries, J., 2006. Diabetes Care 29, 1805–1811.